J Gastroenterol (2016) 51:421–433
DOI 10.1007/s00535-015-1151-3

The Japanese Society of Gastroenterology

REVIEW

Role of contrast-enhanced ultrasonography with Sonazoid for hepatocellular carcinoma: evidence from a 10-year experience

Hitoshi Maruyama[1] · Tadashi Sekimoto[1] · Osamu Yokosuka[1]

Received: 22 September 2015 / Accepted: 25 November 2015 / Published online: 22 December 2015

Abstract Hepatocellular carcinoma (HCC) represents primary liver cancer. Because the development of HCC limits the prognosis as well as the quality of life of the patients, its management should be properly conducted based on an accurate diagnosis. The liver is the major target organ of ultrasound (US), which is the simple, non-invasive, and real-time imaging method available world-wide. Microbubble-based contrast agents are safe and reliable and have become popular, which has resulted in the improvement of diagnostic performances of US due to the increased detectability of the peripheral blood flow. Sonazoid (GE Healthcare, Waukesha, WI, USA), a second-generation contrast agent, shows the unique property of accumulation in the liver and spleen. Contrast-enhanced US with Sonazoid is now one of the most frequently used modalities in the practical management of liver tumors, including the detection and characterization of the nodule, evaluation of the effects of non-surgical treatment, intra-operative support, and post-treatment surveillance. This article reviews the 10-year evidence for contrast-enhanced US with Sonazoid in the practical management of HCC.

Keywords Hepatocellular carcinoma · Contrast-enhanced ultrasound · Sonazoid

Abbreviations

AUROC	Area under the receiver operating characteristic curve
CEUS	Contrast-enhanced ultrasound
CT	Computed tomography
CTA	CT arteriography
CTAP	CT arterioportal angiography
DN	Dysplastic nodule
EOB-MRI	Gadolinium-ethoxybenzyl diethylenetriaminepentaacetic acid-MRI
HCC	Hepatocellular carcinoma
ICC	Intrahepatic cholangiocellular carcinoma
mHCC	Moderately differentiated hepatocellular carcinoma
MIP	Maximum intensity projection
NFLL	New focal liver lesions
NS	Not statistically significant
PR	Partial response
PD	Progressive disease
pHCC	Poorly differentiated hepatocellular carcinoma
RN	Regenerative nodule
RFA	Radiofrequency ablation
SD	Stable disease
S-CEUS	Contrast-enhanced ultrasound with Sonazoid
SPIO-MRI	Superparamagnetic iron oxide magnetic resonance imaging
TACE	Transcatheter arterial chemoembolization
US	Ultrasound
wHCC	Well-differentiated hepatocellular carcinoma

✉ Hitoshi Maruyama
maru-cib@umin.ac.jp

[1] Department of Gastroenterology and Nephrology, Chiba University Graduate School of Medicine, 1-8-1, Inohana, Chuou-ku, Chiba 260-8670, Japan

Introduction

Hepatocellular carcinoma (HCC) represents primary liver cancer [1, 2]. There are many risk factors for HCC occurrence, including the presence of cirrhosis, viral

infection, alcohol intake, and non-alcoholic fatty liver disease. Because the development of HCC limits the prognosis as well as the quality of life of the patients, the importance of the detection, diagnosis, treatment, and post-treatment surveillance of HCC has been emphasized in the clinical management of patients with chronic liver disease.

Because of the advantages of simplicity, noninvasiveness, and real-time observation, ultrasound (US) could be the most frequently used imaging tool for liver diseases. Furthermore, several microbubble-based contrast agents have become available following the introduction of the first-generation microbubble agent Levovist [3, 4]. A harmonic mode enables a high sensitivity for microbubble detection while being less affected by artefact compared with the Doppler mode [2, 5]. Based on these factors, contrast-enhanced US (CEUS) allows stable observation and detailed evaluation of peripheral blood flow in a qualitative and quantitative manner.

Sonazoid (GE Healthcare, Waukesha, WI, USA) is a second-generation contrast agent, and it is available in Japan, South Korea, and Norway (August 2015). The characteristic feature of the agent is the accumulation property in the reticuloendothelial system, such as the liver and spleen [3, 5]. Deep insight has made phase-dependent changes of Sonazoid-induced enhancement to be a major research target, from the earlier phase by circulating microbubbles to the later phase by accumulated microbubbles [5]. A decade has passed since Sonazoid was made clinically available, and a substantial amount of evidence has been accumulated in clinical studies with regard to both non-surgical and surgical management. Furthermore, a recent development of digital technology has introduced a novel presentation beyond 2D sonography—3D imaging under contrast enhancement [4].

This review article focuses on the current clinical application of CEUS with Sonazoid (S-CEUS) for HCC, and it summarizes the 10-year evidence and discusses future directions.

Literature search strategies

The data sources in this review article were international English-based clinical papers in which the research was performed with an appropriate design (clinical study except for case report, adult human research articles) by searching PubMed, MEDLINE, Embase, and ISI Web of Science (Jan 2007–March 2015) using the following keywords: ultrasound/ultrasonography AND HCC/liver tumor AND Sonazoid/perflubutane.

However, the following two papers were exceptionally added to explain the characteristic features of Sonazoid and the phase definition; the paper by Sontum [6] and the paper by Sasaki et al. [7].

Characteristics and safety of Sonazoid

Sonazoid consists of perflubutane microbubbles with a median diameter of 2–3 μm. The concentration was 8 μl/ml by volume and 1×10^9 per milliliter by number [3, 6, 8]. It has the characteristic property of accumulation in the reticuloendothelial systems, being quite different from that of other second-generation contrast agents, SonoVue (Bracco International BV, Amsterdam, The Netherlands) and Definity (Lantheus Medical Imaging, North Billerica, MA, USA) (Table 1) [3]. The Drug Package Insert in Japan indicates a recommended dose of 0.015 ml/kg. However, because this amount was determined based on the data of a premarketing clinical trial a few years earlier, the dose is considered to be excessive for the subsequent US systems which shows improvement in the sensitivity when using microbubbles. Therefore, half of the recommended dose (0.0075 ml/kg) or 0.2 ml per individual is considered to be sufficient for clinical use. The agent is usually administered manually with a bolus injection via peripheral vein, followed by a flush of a certain amount of normal saline.

In general, the incidence of side effects caused by microbubble contrast agents is very low, and that of severe hypersensitivity events is much less than that of iodinated contrast materials [5]. A phase III multicenter clinical trial for Sonazoid performed in Japan showed a 10.4 % (20/193) incidence of adverse drug reactions, and the incidences were mild and nonspecific events in all of the cases [5, 9]. At the same time, according to the Drug Package Insert for Sonazoid in Japan [8], the adverse event and the incidence prior to the approval was diarrhea in 1.0 %, headache in 1.0 %, proteinuria in 0.8 %, the reduction of neutrophil counts in 0.5 %, rash in 0.5 %, dry mouth in 0.5 %, and pain at the injection site in 0.5 %. Heterogeneous staining in the liver parenchyma is a possible event in patients who receive Sonazoid, for 0.77 % of the subjects and in 0.36 % of the examinations [10]. Although the precise mechanism remains unclear, it appears to be harmless to the individual.

Unfortunately, there is only limited data about the use of microbubble contrast agents in cases with pregnancy and pediatrics, especially during breastfeeding. Needless to say, the operators should be trained in resuscitation, and the facilities must be prepared for emergency management.

Phase definition

The contrast-enhanced appearance in the liver changes over time due to the double blood supply from the hepatic artery and portal vein, and the in vivo behavior of the microbubbles. The phases are determined according to the time after the agent injection, 10–20 to 30–45 s for the

Table 1 Second-generation microbubble contrast agents applicable for abdomen

	Sonazoid	SonoVue	Definity
Company	GE Healthcare (Waukesha, WI, USA)	Bracco International BV (Amsterdam, The Netherlands)	Lantheus Medical (Billerica, MA, USA)
Composition	Perfluorobutane	Sulfur hexafluoride	Octafluoropropane
Shell	Phospholipid shell	Phospholipid shell	Lipid shell
Concentration	2–3 μm, 1×10^9/ml	1–12 μm, 2×10^8/ml	1.1–3.3 μm, 1×10^8/ml
Countries[a]	Japan, South Korea, Norway	Europe, others[b]	Canada, Australia

[a] Countries in which the agent is available (August 2015)

[b] Austria, Belgium, Bosnia, Brazil, Bulgaria, China, Croatia, Czech Republic, Denmark, Finland, France, Germany, Greece, Guadeloupe, Hong Kong, Hungary, India, Ireland, Italy, Lebanon, Luxembourg, Monaco, The Netherlands, New Caledonia, Norway, Poland, Portugal, Reunion, Romania, Russia, Saudi Arabia, Singapore, Slovenia, South Korea, Spain, Sweden, Switzerland, UK, USA

arterial phase, 30–45 to 120 s for the portal venous phase, and 120 s to the time of the microbubble disappearance for the late phase [5]. In the S-CEUS, a 10-min phase or later is defined as a post-vascular phase.

The characteristic feature of the Sonazoid is the accumulation property in the reticuloendothelial system like liver and spleen. Although the precise mechanism remains unclear, the trapping of microspheres by the Kupffer cells present in the hepatic parenchyma may be involved in the phenomena [6]. This unique property results in the time-related characteristic changes in the contrast enhancement with Sonazoid. As the Kupffer cells are not present in malignant lesions, the images demonstrate the clear difference of contrast effect between the lesion and surrounding parenchyma.

Actually, accumulation of microbubble would begin immediately after arriving of microbubble in the parenchyma, the phase following portal venous phase could be determined as vasculo-Kupffer phase (1–10 min), which is presented by a time–intensity curve [7]. Thus, the "pure portal venous phase" may be very short in the S-CEUS, determined as the phase from 45 to 60 s after injection [7], and this is a different point between S-CEUS and contrast-enhanced dynamic CT. Nonetheless, the timing of the phases varies according to the microbubble behavior per individual.

Diagnosis

Demonstration of the HCC nodule

Demonstration of the focal hepatic lesion is the initial step in the diagnosis of HCC. A comparison of the detectability of the HCC nodule between S-CEUS and super paramagnetic iron oxide-magnetic resonance imaging (SPIO-MRI) has shown similar sensitivities, 98 % by S-CEUS and 95 % by SPIO-MRI [not statistically significant (NS), 11]. In addition, the dedifferentiation spots of nodule-in-nodule HCCs were detected in 4/5 (80 %) on post-vascular phase images of S-CEUS and in 2/5 (40 %, NS) on SPIO-MRI, which suggests that S-CEUS could be an alternative to SPIO-MRI. The improved detectability of the HCC nodules by S-CEUS is supported by the actual diagnostic values: the sensitivity of the B-mode US was 0.837 and 0.846, and that of S-CEUS was 0.732 and 0.831, and the specificity of the B-mode US was 0.902 and 0.949 and that of S-CEUS was 0.986 and 0.978, for readers A and B, respectively [12]. Misidentification of hepatic cysts was the main reason for false-positive results by S-CEUS [12]. A clear visualization of the macroscopic type of HCC nodule with a conspicuous border line is another benefit of using S-CEUS [13–15].

Assessment of the tumor vascularity

The detectability of tumor vascularity in HCC nodules by S-CEUS is equal to that of contrast-enhanced computed tomography CT [16] or is more sensitive [17]. The other study showed that S-CEUS detected hypervascularity in seven of the 27 HCC nodules that have a non-hyper vascular appearance on contrast-enhanced CT [18]. Subsequent biopsy proved evidence for HCC in all of them, which suggests the significance of S-CEUS in such cases. At the same time, there is another issue, which is the source of the blood supply in the HCC. According to the study by Kudo et al. [19], pure arterial phase imaging by a maximum intensity projection (MIP) technique enables us to determine whether the tumor blood supply is arterial or portal in origin, which can facilitate the noninvasive characterization of the lesions in cirrhosis. The characteristic corona enhancement, which probably reflects portal drainage of HCC, is also a possible target of S-CEUS due to real-time observation with a higher spatial resolution [20].

Characterization of focal hepatic lesions

The clinical value of the imaging modality depends on the substantial diagnostic performance, and the characterization of focal hepatic lesions could be an issue in which CEUS plays an important role.

Arterial hyper-vascularity could feature a typical finding of HCC [1, 18, 21] (Fig. 1), and the vascular pattern on S-CEUS is effective for differentiating between early HCC and the regenerative nodule (RN) [22]. The enhancement pattern at the 5-min phase or later is also useful in characterizing various hepatic nodules (a total of 208 nodules; HCC, meta, hemangioma, and focal nodular hyperplasia) with 75–85 % sensitivity, 88–100 % specificity, and 85–92 % positive predictive value [23].

A comparison of the diagnostic ability for hepatic nodules (a total of 113 nodules; HCC, metastatic tumor, intrahepatic cholangiocellular carcinoma [ICC], dysplastic nodule [DN]) between S-CEUS and contrast-enhanced CT showed that the sensitivity and accuracy was significantly higher in the former (95.4, 94.7 %) than in the latter (85.2, 82.3 %) [24]. The other study reported that the sensitivity and specificity of S-CEUS for HCC diagnosed by contrast-enhanced CT was 94.7 and 81.8 %, respectively [25]. The study also diagnosed two liver tumors that were detected by S-CEUS but not by contrast-enhanced CT; biopsies revealed one tumor to be a well-differentiated HCC (wHCC) and the other to be an atypical adenomatous hyperplasia.

According to the study by Takahashi et al., the area under the receiver operating characteristic curve (AUROC) to identify wHCC was higher in the arterial phase in S-CEUS (0.8316) than with gadolinium-ethoxybenzyl diethylenetriaminepentaacetic acid (EOB)-MRI (0.6659, $p = 0.0101$) and similar in the liver-specific phase in S-CEUS (0.7225) and EOB-MRI (0.7347, $p = 0.8814$) [26]. The authors concluded that hypervascularity is a significant feature that distinguishes wHCC from RN, and S-CEUS exerts a beneficial impact better than EOB-MRI for such characterization. However, both imaging methods have comparable abilities in the characterization of non-hypervascular lesions, and they compensate mutually for the poor sensitivity of S-CEUS and the poor specificity of EOB-MRI in the liver-specific phase. A similar diagnostic ability for HCC between S-CEUS and EOB-MRI is also supported by the other studies [27, 28]. The sensitivity in 34 HCC nodules (<2 cm) in the study by Mita et al. was 88.2 % by CT arterioportal angiography (CTAP), 76.5 % by EOB-MRI, 67.6 % by S-CEUS and 52.9 % by contrast-enhanced CT, with no significant difference between CTAP, EOB-MRI, and S-CEUS. As expected, the combined methods can provide much better results; the sensitivity was 94.1 % (32/34) by S-CEUS and EOB-MRI [27], 90 % by S-CEUS and EOB-MRI, 82 % by S-CEUS and contrast-enhanced CT, and 88 % by contrast-enhanced CT and EOB-MRI [29]. However, a more recent study suggests that an uptake of Sonazoid starts decreasing later than that of EOB-MRI and that a hypoechoic appearance on the post-vascular phase of S-CEUS might be specific to HCC rather than EOB-MRI, especially in the progressed HCC [30]. The sensitivity/specificity of the modality depends on the patient population (Figs. 2, 3); nevertheless, recent

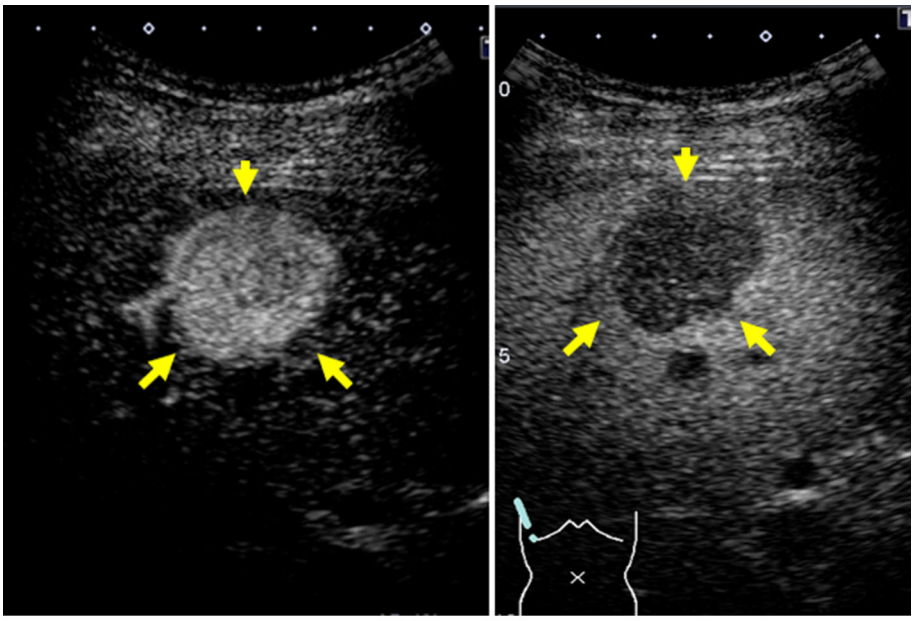

Fig. 1 A 79-year old male, hepatitis C virus-related cirrhosis, segment 5, moderately-differentiated hepatocellular carcinoma, 30 mm. **a** Arterial phase, 21 s after the agent injection. The image shows hyper-enhancement in the hepatic nodule (*arrows*). **b** Post-vascular phase, 15 m after the agent injection. The image shows hypo-enhancement in the hepatic nodule (*arrows*)

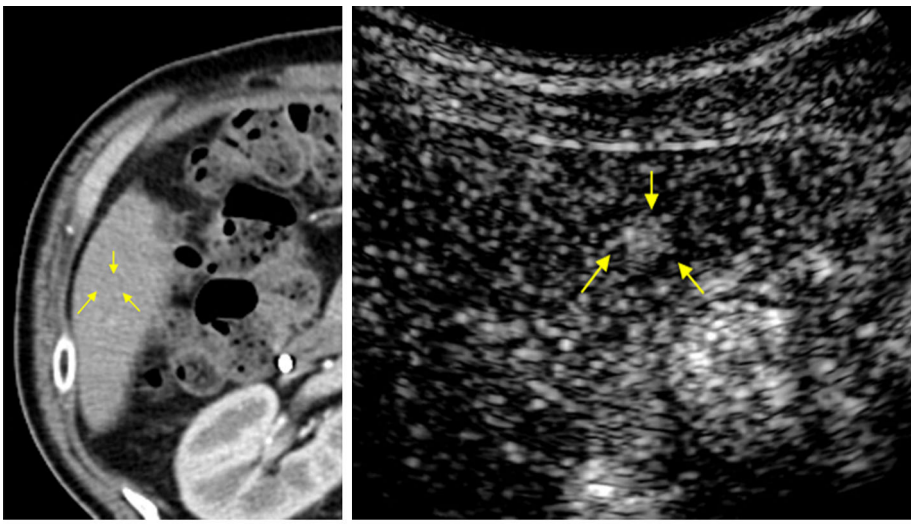

Fig. 2 Comparison of intra-tumor contrast enhancement between S-CEUS and contrast-enhanced CT 75-year-old male, hepatitis B virus-related cirrhosis, segment 6, well-differentiated hepatocellular carcinoma, 11 mm. **a** CT, arterial phase. The image shows iso-enhancement in the nodule (*arrows*). **b** S-CEUS, arterial phase (40 s after the agent injection). The nodule shows clear hyper-enhancement (*arrows*). *S-CEUS* contrast-enhanced ultrasound with Sonazoid; *CT* computed tomography

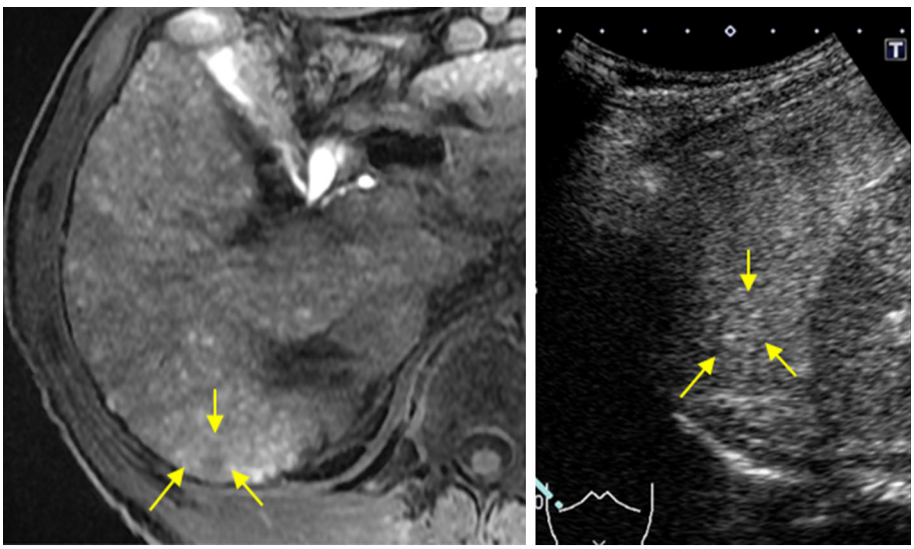

Fig. 3 Comparison of intra-tumor contrast enhancement between S-CEUS and EOB-MRI in a 57-year-old male, alcoholic cirrhosis, segment 6, well-differentiated hepatocellular carcinoma, 10 mm. **a** EOB-MRI, hepatobiliary phase. The image shows hypo-enhancement in the nodule (*arrows*). **b** S-CEUS, post-vascular phase. The image shows iso-enhancement in the nodule (*arrows*). S-CEUS, contrast-enhanced ultrasound with Sonazoid. EOB-MRI, gadolinium-ethoxybenzyl diethylenetriaminepentaacetic acid magnetic resonance imaging

evidence has strongly indicated that the diagnostic ability of S-CEUS for HCC is at least the same as that of EOB-MRI.

Cellular differentiation

The understanding of multistep carcinogenesis serves as a platform for imaging diagnosis of cellular differentiation of HCC [31]. The integrated assessment of both the arterial phase and post-vascular phase could be a common procedure in the prediction of cellular differentiation, represented by the degree of enhancement in both phases [32] or the intra-tumor vascular appearance demonstrated by MIP and post-vascular phase enhancement (20 min) [33]. Kondo et al. [34] examined the AUROC of the phase-related intensity parameters for discriminating between wHCC and moderately differentiated HCC (mHCC), 0.6922 for the arterial phase, 0.7680 for post-vascular phase, and 0.7925 for the integrated parameter of both phases, which showed the highest performance. Although the data suggests the advantage of the combined use of both phases, further improvement in the diagnostic ability is required because the value of the AUROC remains insufficient.

Which precedes the dedifferentiation process of HCC, an early phase enhancement due to a vascularity change or a reduction in the microbubble accumulation? This question could arise when phase-related contrast effects are evaluated. One study gives us the answer that changes in tumor vascularity precede microbubble contrast

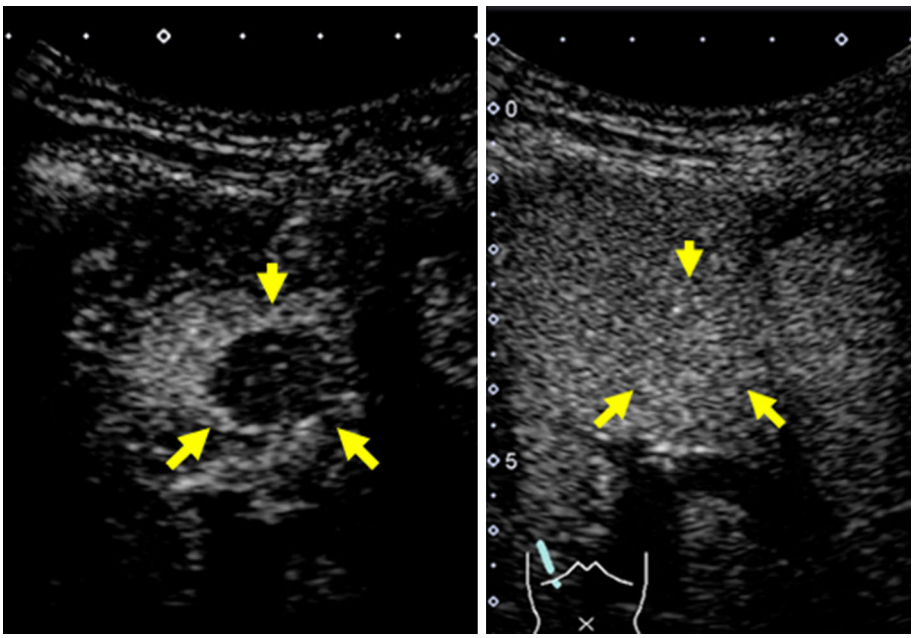

Fig. 4 A 73-year old male, hepatitis C virus-related cirrhosis, segment 4, well-differentiated hepatocellular carcinoma, 12 mm. **a** Arterial phase, 27 s after the agent injection. The image shows hypo-enhancement in the hepatic nodule (*arrows*). **b** Post-vascular phase, 11 m after the agent injection. The image shows iso-enhancement in the hepatic nodule (*arrows*)

accumulation deficit in the process of dedifferentiation of HCC [35]. Therefore, the observation of the vascular phase could be more effective than that of the post-vascular phase imaging for the early recognition of HCC dedifferentiation when using S-CEUS. For the visualization of dynamic changes in the contrast effect, Takahashi et al. [36] focused on the timing of "wash out" during the contrast enhancement in 77 histologically proven HCC nodules; washout was more frequent in poorly-differentiated HCC (pHCC) than in mHCC ($p = 0.0117$) and wHCC ($p = 0.0003$) in the 1-min phase and was more frequent in mHCC than in wHCC in the 5-min ($p = 0.0026$) and 10-min ($p = 0.0117$) phases, which indicates the predictive value of the cellular differentiation.

The other study compared the AUROC between the post-vascular phase images of S-CEUS and liver-specific phase images of EOB-MRI, which resulted in 0.705 and 0.785 for DN versus wHCC, mHCC and pHCC ($p = 0.517$), 0.791 and 0.687 for DN and wHCC versus mHCC and pHCC ($p = 0.093$), and 0.871 and 0.716 for DN and w/mHCC versus pHCC ($p = 0.005$), respectively [37]. The data strongly suggest that there is an advantage of S-CEUS over EOB-MRI in the diagnosis of mHCC or pHCC.

At the same time, iso-enhancement in the post-vascular phase could have a confusing appearance because it is detected in both wHCC and borderline nodules [2, 4, 26, 36] (Fig. 4). A recent study examined the natural history of iso-enhanced lesions and found that lesions of >14 mm with iso-enhancement in the post-vascular phase should be carefully monitored because of the high potential of HCC occurrence [38].

Because of the characteristics of Sonazoid, the degree of microbubble accumulation could reflect the morphological findings of the HCC nodules [39]. This speculation is partially supported by a study that focused on the heterogeneity of the intra-nodular enhancement at the post-vascular phase, which suggested the relationship between the variability in the distribution of accumulated microbubbles and the tissue differences in the wHCC and RN [40]. However, the scientific connection between the post-vascular phase enhancement and histological degree of malignancy does not go beyond speculation, and characterization of borderline hepatic nodules remains difficult at present [41].

Treatment

Detection of HCC nodule unidentified by conventional B-mode US

Detection of the target lesion is essential to achieving US-guided local treatment, and CEUS could exert a beneficial effect for this purpose [4, 42]. The detectability by S-CEUS for a nodule that is not identified by conventional B-mode US is summarized in Table 2, and it shows excellent results for 93–100 % [43–47]. Basically, a post-vascular image is applied to identify the nodule based on the enhancement differences, positive microbubble accumulation in the

Table 2 Detection of HCC nodule, which is not identified by conventional B-mode ultrasound

N	Lesion (untreated/recurrence)	Size (mm)	Vascularity	Phase	Detectability	Author
55	Untreated/recurrence	5–24	Hyper (CT)	Early/post-vascular	53/55 (96 %)	Maruyama [43]
17	Local recurrence	10–25	Hyper (CT)	Post-vascular/re-injection	17/17 (100 %)	Miyamoto [44]
15 (108)	Untreated/recurrence	7–98	Hyper (CT)	Early/post-vascular	14/15 (93 %)	Numata [45]
61 (108)	Untreated/recurrence	7–35	Hyper (CT)	Post-vascular/re-injection	61/61 (100 %)	Minami [46]
67	Untreated/recurrence	–	Hyper (CT)	Post-vascular/re-injection	67/67 (100 %)	Kudo [47]

HCC hepatocellular carcinoma, *N* number of HCC nodule (total number of hepatic nodule), *CT* computed tomography

surrounding liver parenchyma, and negative accumulation in the HCC nodules due to the lack of a reticuloendothelial system. However, it can be argued that both the treated and untreated HCC nodules could show negative enhancement in this phase, therefore discrimination between them may be difficult. In this regard, Kudo et al. [48] reported a unique technique that involved re-injection of Sonazoid for lesions at the post-vascular phase, which is called "defect reperfusion US imaging"; this approach is effective at confirming the vascularity/viability in nodules that show post-vascular phase negative enhancement.

Radiofrequency ablation (RFA)

Radiofrequency ablation (RFA) could be the most frequently used local treatment for HCC, and it has a curative effect which is similar to that of surgical resection [49, 50].

The practical benefits of S-CEUS for RFA treatment have been described in recent studies; the first study shows that the introduction of S-CEUS increased the percentage of RFA-applicable cases from 21 % ($n = 95$) to 32 % ($n = 219$) in total and from 32 % ($n = 41$) to 52 % ($n = 89$) for naïve subjects ($p < 0.01$) [51]. The next study demonstrated that S-CEUS reduces the number of RFA sessions, 1.33 ± 0.45 versus 1.49 ± 0.76 (historical controls, $p = 0.0019$) [52]. Third, better radicality was attained [53, 54] with a higher non-local recurrence rate (92.1 % at 1 year, and 85.3 % at 2 years versus 76.3 % at 1 year and 66.4 % at 2 years) [53].

A comparison of the pre- and post-RFA images allows the assessment of a therapeutic effect [4, 54], and therefore, S-CEUS could have the potential to reduce the number of CT examinations [55]. A more recent study has shown that S-CEUS performed 3 h after RFA could recognize the outline of the coagulated tumors in 78/87 patients (89.7 %), and the 5-year cumulative local recurrence rate was very low (2.3 %), with a 5-year cumulative survival rate of 58.4 % [56].

In spite of the application of RFA with various measures by expertise [57], still some of the patients suffer from post-treatment recurrence [58]. There are two risky signs for recurrence. The first sign is a linear-shaped positive enhancement, which was demonstrated in the RFA-treated area in 33 lesions (18.4 %) by S-CEUS; 17 of them were followed up with no treatment, and 3/17 (17.6 %) showed a local tumor progression that corresponded to linear enhancement [59]. Although there was not a significant difference in the local recurrence rate between lesions with linear enhancement (3/17) and without linear enhancement (10/35), the local tumor progression inside the ablation zone occurred only in the lesions that had linear enhancement. The next is the intra-tumor gradual enhancement in the pre-treatment early arterial phase, which indicates potential risk for a distant recurrence after RFA [60]. Taken together, careful post-treatment surveillance could be required in patients with these findings.

Transcatheter arterial chemoembolization (TACE)

TACE is the interventional treatment for HCC that is performed in many countries [1]. It is usually applied to patients who have multiple HCC nodules, beyond the stage for a local curative treatment. One of the interests of clinicians has been the early prediction of the therapeutic effect. To better understand the proper way of the assessment, a study compared the detection rates of residual tumors between the two modalities, S-CEUS and CT, both at 1 week after TACE, and found that the former was more sensitive than the latter (58.1 vs. 39.5 %; $p < 0.01$) [61]. The prospective study that was performed later showed that the detection rate for residual HCC nodules using S-CEUS 1 day after TACE (95.7 %, 45/47) was significantly higher than that using contrast-enhanced CT 1 month after TACE (78.7 %, 37/47; $p < 0.05$) [62]. It is considered that the lower influence of iodized oil-induced artefacts, which affects the evaluation of CT images, accounts for the higher sensitivity of S-CEUS for detecting the residual viable HCC.

Sorafenib

Sorafenib (Bayer, Leverkusen, Germany) is the first oral multikinase inhibitor, and it has been approved for the treatment of advanced unresectable HCC [63]. Because

one of the targets of Sorafenib is angiogenesis (vascular endothelial growth factor receptor and platelet-derived growth factor receptor), there is a hypothesis that the evaluation of hepatic hemodynamics using CEUS could have a potential effect on the prediction of the therapeutic results. Two studies assessed the therapeutic effect of Sorafenib from the aspect of S-CEUS findings; the first study examined the mean arrival time of Sonazoid using parametric imaging [64]. Differences in the arrival time between the stable disease (SD), partial response (PR) and progressive disease (PD) groups were significant in 2 weeks ($p = 0.019$) and 4 weeks ($p = 0.028$) after the treatment. The next study was performed in 37 HCC patients and reported that changes in the perfusion parameters in the tumor and liver parenchyma can be useful for the early prediction of tumor response and major adverse events in patients with HCC [65]. Obviously, a precise and early prediction of a therapeutic effect would offer the direction of medical care, maintain the current treatment, or facilitate the adaption of the next management. However, there are only a few studies that include heterogeneous patient characteristics; therefore, we are underpowered to address a definitive conclusion. More data are needed to confirm the benefit of S-CEUS in this regard.

Surgical application

Investigators have shown the benefit of intra-operative S-CEUS on the diagnosis of HCC and safety improvement [66–68] (Table 3).

A prospective study that included 192 patients reported that 79 new focal liver lesions found during the fundamental intraoperative US (fundamental-NFLLs) were detected in 50 patients (26 %), 17 (22 %) of which were finally diagnosed as HCC [69]. The sensitivity, specificity, and accuracy of intraoperative S-CEUS for differentiating HCC among fundamental-NFLLs were 65, 94, and 87 %, respectively. In addition, the intraoperative S-CEUS identified 21 additional new hypoechoic lesions in 16 patients, of which 14 lesions (67 %) in 11 patients were finally diagnosed as HCC.

The diagnostic ability of intraoperative S-CEUS in the detection of the HCC nodule is comparable to that of preoperative CT arteriography (CTA), with a sensitivity of (S-CEUS 97.6 %, CTA 89.4 %) and positive predictive value of (S-CEUS 91.2 %, CTA 91.6 %) in reference to the standard of surgically resected specimen [70].

Similar to the results by transabdominal S-CEUS, two-phase enhancement patterns (arterial-phase vascularity and post-vascular phase enhancement) by intraoperative S-CEUS are predictive of the histological appearance [71]. A more recent study proved the relationship between the intra-tumor vascular pattern on intraoperative S-CEUS and poor prognosis via gene expression of geminin in HCC patients [72].

Although liver transplantation is now a definite option for end-stage liver disease with/without HCC, there is a lack of evidence in the role of S-CEUS. It would be challenging to design studies to examine the effect of S-CEUS on the pre-operative evaluation of the donor and recipient, intra-operative assessment and post-operative surveillance.

3D images

Marked development of digital technology has dramatically introduced 3D visualization of US imaging (Fig. 5). Characteristic vascular appearance in the hepatic nodules could be clearly demonstrated by the 3D S-CEUS with a sufficient inter-reviewer agreement [73, 74]. The same group reported the utility of 3D S-CEUS for the immediate evaluation of the therapeutic effect of extracorporeal high-intensity focused ultrasound ablation in HCC nodules with 100 % sensitivity, 75 % specificity, and 95 % accuracy [75].

More recently, the demonstration of combined images with US and other modalities has become available on the same display and is called “fusion imaging” (Fig. 6). According to the prospective study by Kunishi et al. [76], the detection rate of small HCCs (1–2 cm) was significantly higher in the fusion imaging using conventional US and EOB-MRI (97 %, 59/61) compared with the conventional US (66 %, 40/61) and S-CEUS (80 %, 49/61) ($p < 0.01$, for both). In addition, the detection rate for atypical HCCs was also significantly higher using fusion imaging (95 %, 18/19) compared with using conventional US (53 %, 10/19) and S-CEUS (26 %, 5/19) ($p < 0.01$, for both) [76]. The benefit of the fusion imaging for RFA treatment has been proven to be a significant reduction with poor conspicuity on grayscale US (1.7 %, 2/120 vs. 15.4 %, 19/123, $p < 0.01$) [77]. Moreover, a Korean study reported that fusion imaging with S-CEUS and CT/MRI was highly effective in performing RFA for very early-stage HCCs inconspicuous on fusion imaging with B-mode US and CT/MRI [78].

Numata et al. prospectively examined the effect of fusion imaging that combines S-CEUS and contrast-enhanced CT images to evaluate the therapeutic effect in 80 HCC nodules (1–3 cm) 1 day after the RFA [79]. When the 1-month contrast-enhanced CT images were used as a reference standard, the sensitivity, specificity, and accuracy of the 1-day fusion imaging for the diagnosis of adequate ablation were 97, 83, and 96 %, respectively, which suggests the usefulness of early evaluation of the RFA effect

Table 3 Utility of intra-operative contrast-enhanced ultrasound with Sonazoid for HCC

N	Vascularity	Diagnostic ability	Detection of additional tumor	Surgical margin	Authors
111	–	Se98 %, Sp83 %, PPV99 %, NPV71 %, Ac97 %†	–	–	Abo [66]
83 (52)	–	Se97.6 % (CTA89.4 %), PPV91.2 % (CTA91.6 %)†	8 nodules	–	Mitsunori [70]
79 (50)	–	Se65 %, Sp94 %, Ac87 %†	21 nodules (14/21, HCC)	–	Arita [69]
374	186/239 (78 %)	wHCC versus mHCC/pHCC*	–	–	Arita [71]
25	23/25 (92 %)	–	1 nodule (8 mm)	0/25 versus 4/40** ($p = 0.073$)	Nanashima [68]

N number of HCC nodule (number of patient), *HCC* hepatocellular carcinoma, *wHCC* well-differentiated HCC, *mHCC* moderately differentiated HCC, *pHCC* poorly differentiated HCC, *Se* sensitivity, *Sp* specificity, *PPV* positive predictive value, *NPV* negative predictive value, *Ac* accuracy, *CTA* computed tomography under arteriography

* Hypervascular, wHCC (66 %) versus mHCC/pHCC (80 %), $p = 0.058$. Hypo-enhancement at the post-vascular phase, wHCC (54 %) versus mHCC/pHCC (92 %), $p < 0.0001$

** Negative margin in 25 nodules by contrast-enhanced ultrasound with Sonazoid but positive margin in four nodules by conventional B-mode ultrasound

† Malignant versus benign tumor

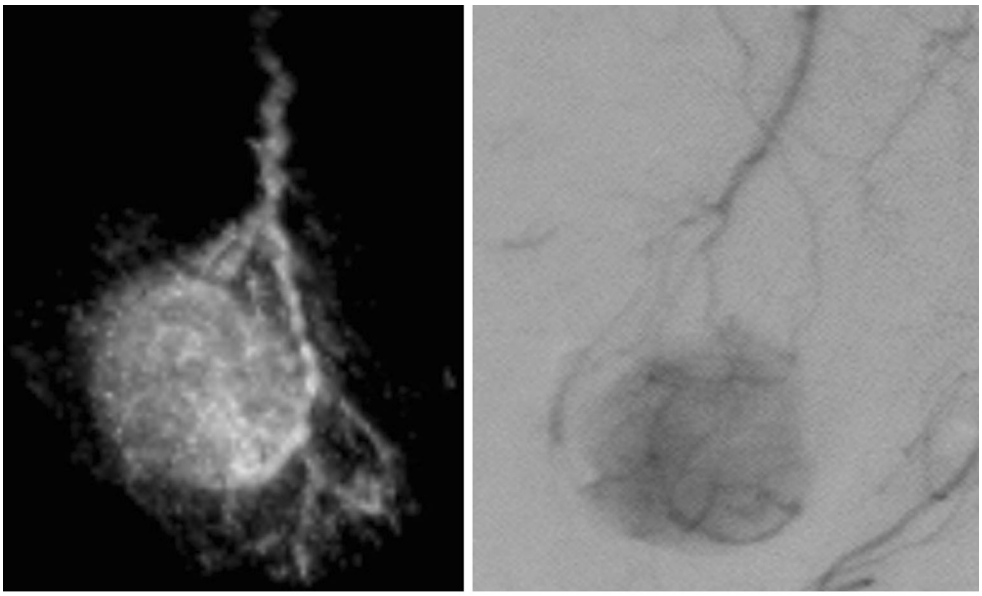

(A) **(B)**

Fig. 5 Contrast-enhanced three-dimensional image (maximum intensity projection) using Sonazoid for hepatocellular carcinoma (54-year-old male, hepatitis C virus-related cirrhosis, segment 6, hepatocellular carcinoma, 27 mm). The three-dimensional image (**a**) clearly demonstrates the tumor vessels, similar to those by hepatic arteriography (**b**)

by fusion imaging. The application of 3D S-CEUS is also effective in the intra-operation setting for the staging of anatomic liver resection [80]. These data strongly suggest that the 3D approach would open the new possibility of using CEUS to overcome the limitations of 2D-based visualizations.

Challenges and prospects

Management of HCC has greatly improved over the past few years with the contribution of S-CEUS, as described in this review article. However, there are still some issues which must be addressed.

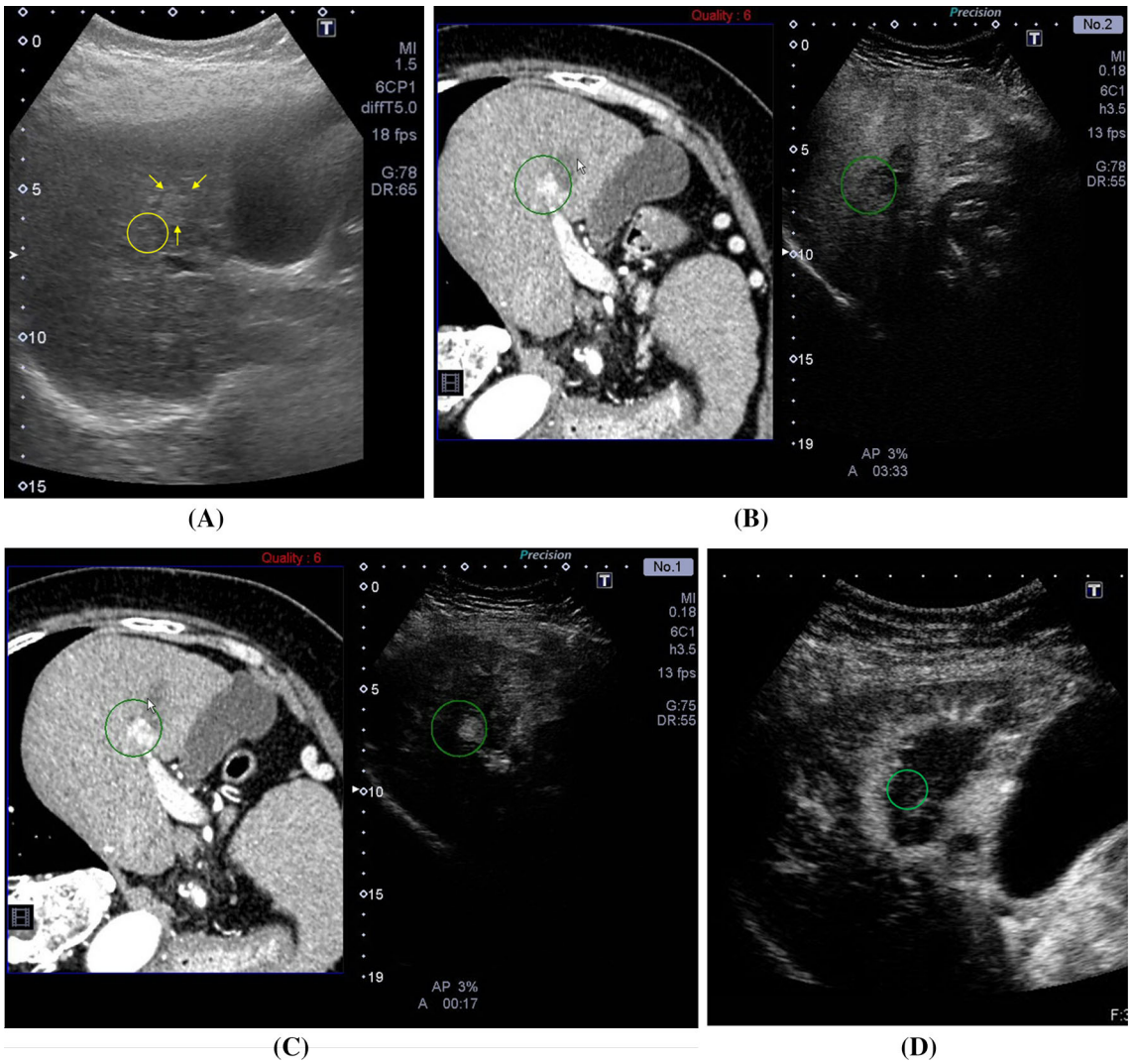

Fig. 6 Fusion imaging for the recurrent hepatocellular carcinoma nodule, which was not identified by conventional B-mode ultrasound in a 71-year-old female, cirrhosis (nonalcoholic steatohepatitis), segment 5, hepatocellular carcinoma, 15 mm. **a** B-mode. The image shows post-treatment lesion by radiofrequency ablation (*arrows*). The actual viable tumor detected by subsequent fusion imaging is indicated by a sphere, which was not identified with B-mode sonography. **b** Fusion imaging, post-vascular phase. The viable lesion adjacent to the post-treatment lesion was detected as a hypo-enhanced area on the sonogram (*right panel, circle*). *Left image*, contrast-enhanced computed tomography. *Right image*, S-CEUS at the post-vascular phase. **c** Fusion imaging, arterial phase. Hypervascular nodule was clearly demonstrated using fusion imaging, indicating the definitive finding of viable lesion (*circle*). *Left image*, contrast-enhanced computed tomography. *Right image*, S-CEUS at the arterial phase. **d** S-CEUS after RFA. RFA was successfully performed for the recurrent lesion detected by fusion imaging. The arterial-phase sonogram showed no enhancement in the recurrent nodule (*circle*), suggesting successful treatment. S-CEUS, contrast-enhanced ultrasound with Sonazoid. RFA, radiofrequency ablation

First, according to the global trend that enhances the need for less-invasive procedures to reduce the burden of the patients, the guidelines for HCC management emphasize the value of imaging findings and limit the applications of biopsies [1, 81]. However, CEUS is recommended with the diagnostic algorithm in only Asian and Italian guidelines [81]. This limitation would be important to overcome in the near future, considering the digital technology developments and increasing knowledge, which would further increase the impact of the technique.

Second is the cost-effectiveness; Tanaka et al. [82] reported that HCC surveillance by S-CEUS is a cost-effective strategy for cirrhosis patients and gains them the longest additional life years, with a similar degree of incremental cost effectiveness ratio in the US surveillance group. However, the power depends on the economic conditions, which could vary over time, and the substantial effect has yet to be evaluated in each country. In addition, it is a permanent issue that the reduction of medical care cost must be continuously considered by seeking better methods for surveillance.

Third is the disadvantages of CEUS due to the nature of US. The major drawback is the presence of blind area such as the lateral angle of the liver, which may be overcome using postural change and/or artificial pleural effusion/ascites in most cases. Although it is suggested that S-CEUS is less affected by the observer's experience and is more accurate in the diagnosis of local recurrence after the treatment for HCC compared with contrast-enhanced CT [83], the operator-dependency is also considerable issue. Additionally, the assessment of the degree of vascularity in the early phase is not always easy particularly in the small nodules, because it is the time-limited dynamic phase and subsequent parenchymal enhancement may overlay the contrast effect in the hepatic lesions. It is important that clinicians should be aware of these potential pitfalls and make the decision to leave the diagnosis in the other imaging modalities. Needless to say, certain skills, knowledge, and experience would be more or less required when performing CEUS, and a specific training system must be created for the further prevalence of CEUS.

Finally, the availability of Sonazoid in a limited number of countries could be an impediment that motivates the accumulation of further clinical evidence.

Conclusions

This comprehensive review clearly demonstrates the magnitude of the importance of S-CEUS in the management of HCC. Theoretically, because it is less invasive and highly beneficial, this approach would offer a major role in the detailed diagnostics in addition to being a first-line imaging tool. Continuous research efforts will surely help to provide an internationally recognized position for CEUS, which results in further improvement of the outcomes of patients with HCC.

Compliance with ethical standards

Conflict of interest The authors declare that they have no conflict of interest.

References

1. Kudo M, Matsui O, Izumi N, Liver Cancer Study Group of Japan, et al. Surveillance and diagnostic algorithm for hepatocellular carcinoma proposed by the Liver Cancer Study Group of Japan: 2014 update. Oncology. 2014;87(Suppl 1):7–21.
2. Jang HJ, Kim TK, Burns PN, et al. CEUS: an essential component in a multimodality approach to small nodules in patients at high-risk for hepatocellular carcinoma. Eur J Radiol. 2015;84:1623–35.
3. Bouakaz A, de Jong N. WFUMB Safety Symposium on Echo-Contrast Agents: nature and types of ultrasound contrast agents. Ultrasound Med Biol. 2007;33:187–96.
4. Numata K, Luo W, Morimoto M, et al. Contrast-enhanced ultrasound of hepatocellular carcinoma. World J Radiol. 2010;2:68–82.
5. Claudon M, Dietrich CF, Choi BI, et al. Guidelines and good clinical practice recommendations for contrast enhanced ultrasound (CEUS) in the liver—update 2012: a WFUMB-EFSUMB initiative in cooperation with representatives of AFSUMB, AIUM, ASUM, FLAUS and ICUS. Ultrasound Med Biol. 2013;39:187–210.
6. Sontum PC. Physicochemical characteristics of SonazoidTM, a new contrast agent for ultrasound imaging. Ultrasound Med Biol. 2008;34:824–33.
7. Sasaki S, Iijima H, Moriyasu F, Hidehiko W. Definition of contrast enhancement phases of the liver using a perfluoro-based microbubble agent, perflubutane microbubbles. Ultrasound Med Biol. 2009;35:1819–27.
8. Drugs in Japan forum. Drugs in Japan, ethical drugs 2011. Tokyo: Jiho; 2010.
9. Moriyasu F, Itoh K. Efficacy of perflubutane microbubble-enhanced ultrasound in the characterization and detection of focal liver lesions: phase 3 multicenter clinical trial. AJR Am J Roentgenol. 2009;193:86–95.
10. Shimada T, Maruyama H, Sekimoto T, et al. Heterogeneous staining in the liver parenchyma after the injection of perflubutane microbubble contrast agent. Ultrasound Med Biol. 2012;38:1317–23.
11. Inoue T, Kudo M, Hatanaka K, et al. Imaging of hepatocellular carcinoma: qualitative and quantitative analysis of post vascular phase contrast-enhanced ultrasonography with Sonazoid. Comparison with super paramagnetic iron oxide magnetic resonance images. Oncology. 2008;75(Suppl 1):48–54.
12. Goto E, Masuzaki R, Tateishi R, et al. Value of post-vascular phase (Kupffer imaging) by contrast-enhanced ultrasonography using Sonazoid in the detection of hepatocellular carcinoma. J Gastroenterol. 2012;47:477–85.
13. Hatanaka K, Chung H, Kudo M, et al. Usefulness of the post-vascular phase of contrast-enhanced ultrasonography with Sonazoid in the evaluation of gross types of hepatocellular carcinoma. Oncology. 2010;78(Suppl 1):53–9.
14. Tada T, Kumada T, Toyoda H, et al. Utility of contrast-enhanced ultrasound with perflubutane for diagnosing the macroscopic type of small nodular hepatocellular carcinomas. Eur Radiol. 2014;24:2157–66.
15. Hatanaka K, Minami Y, Kudo M, et al. The gross classification of hepatocellular carcinoma: usefulness of contrast-enhanced US. J Clin Ultrasound. 2014;42:1–8.
16. Mandai M, Koda M, Matono T, et al. Assessment of hepatocellular carcinoma by contrast-enhanced ultrasound with perfluorobutane microbubbles: comparison with dynamic CT. Br J Radiol. 2011;84:499–507.
17. Numata K, Fukuda H, Miwa H, et al. Contrast-enhanced ultrasonography findings using a perflubutane-based contrast agent in patients with early hepatocellular carcinoma. Eur J Radiol. 2014;83:95–102.
18. Maruyama H, Takahashi M, Ishibashi H, et al. Contrast-enhanced ultrasound for characterisation of hepatic lesions appearing non-hypervascular on CT in chronic liver diseases. Br J Radiol. 2012;85:351–7.
19. Kudo M, Hatanaka K, Inoue T, et al. Depiction of portal supply in early hepatocellular carcinoma and dysplastic nodule: value of pure arterial ultrasound imaging in hepatocellular carcinoma. Oncology. 2010;78(Suppl 1):60–7.
20. Kita R, Sakamoto A, Nagata Y, et al. Visualization of blood drainage area from hypervascular hepatocellular carcinoma on ultrasonographic images during hepatic arteriogram: comparison

with depiction of drainage area on contrast-enhanced ultrasound. Hepatol Res. 2012;42:999–1007.
21. Sugimoto K, Shiraishi J, Moriyasu F, et al. Computer-aided diagnosis of focal liver lesions by use of physicians' subjective classification of echogenic patterns in baseline and contrast-enhanced ultrasonography. Acad Radiol. 2009;16:401–11.
22. Numata K, Fukuda H, Nihonmatsu H, et al. Use of vessel patterns on contrast-enhanced ultrasonography using a perflubutane-based contrast agent for the differential diagnosis of regenerative nodules from early hepatocellular carcinoma or high-grade dysplastic nodules in patients with chronic liver disease. Abdom Imaging. 2015;40:2372–83.
23. Luo W, Numata K, Kondo M, et al. Sonazoid-enhanced ultrasonography for evaluation of the enhancement patterns of focal liver tumors in the late phase by intermittent imaging with a high mechanical index. J Ultrasound Med. 2009;28:439–48.
24. Hatanaka K, Kudo M, Minami Y, et al. Sonazoid-enhanced ultrasonography for diagnosis of hepatic malignancies: comparison with contrast-enhanced CT. Oncology. 2008;75(Suppl 1):42–7.
25. Kan M, Hiraoka A, Uehara T, et al. Evaluation of contrast-enhanced ultrasonography using perfluorobutane (Sonazoid®) in patients with small hepatocellular carcinoma: comparison with dynamic computed tomography. Oncol Lett. 2010;1:485–8.
26. Takahashi M, Maruyama H, Shimada T, et al. Characterization of hepatic lesions (≤30 mm) with liver-specific contrast agents: a comparison between ultrasound and magnetic resonance imaging. Eur J Radiol. 2013;82:75–84.
27. Mita K, Kim SR, Kudo M, et al. Diagnostic sensitivity of imaging modalities for hepatocellular carcinoma smaller than 2 cm. World J Gastroenterol. 2010;16:4187–92.
28. Kawada N, Ohkawa K, Tanaka S, et al. Improved diagnosis of well-differentiated hepatocellular carcinoma with gadolinium ethoxybenzyl diethylene triamine pentaacetic acid-enhanced magnetic resonance imaging and Sonazoid contrast-enhanced ultrasonography. Hepatol Res. 2010;40:930–6.
29. Alaboudy A, Inoue T, Hatanaka K, et al. Usefulness of combination of imaging modalities in the diagnosis of hepatocellular carcinoma using Sonazoid®-enhanced ultrasound, gadolinium diethylene-triamine-pentaacetic acid-enhanced magnetic resonance imaging, and contrast-enhanced computed tomography. Oncology. 2011;81(Suppl 1):66–72.
30. Ohama H, Imai Y, Nakashima O, et al. Images of Sonazoid-enhanced ultrasonography in multistep hepatocarcinogenesis: comparison with Gd-EOB-DTPA-enhanced MRI. J Gastroenterol. 2014;49:1081–93.
31. Kudo M. Multistep human hepatocarcinogenesis: correlation of imaging with pathology. J Gastroenterol. 2009;44(Suppl 19):112–8.
32. Suzuki K, Okuda Y, Ota M, et al. Diagnosis of hepatocellular carcinoma nodules in patients with chronic liver disease using contrast-enhanced sonography: usefulness of the combination of arterial- and Kupffer-phase enhancement patterns. J Ultrasound Med. 2015;34:423–33.
33. Tanaka H, Iijima H, Higashiura A, et al. New malignant grading system for hepatocellular carcinoma using the Sonazoid contrast agent for ultrasonography. J Gastroenterol. 2014;49:755–63.
34. Kondo T, Maruyama H, Kiyono S, et al. Intensity-based assessment of microbubble-enhanced ultrasonography: phase-related diagnostic ability for cellular differentiation of hepatocellular carcinoma. Ultrasound Med Biol. 2015;41:3079–87.
35. Maruyama H, Takahashi M, Ishibashi H, et al. Changes in tumor vascularity precede microbubble contrast accumulation deficit in the process of dedifferentiation of hepatocellular carcinoma. Eur J Radiol. 2010;75:e102–6.
36. Takahashi M, Maruyama H, Ishibashi H, et al. Contrast-enhanced ultrasound with perflubutane microbubble agent: evaluation of differentiation of hepatocellular carcinoma. AJR Am J Roentgenol. 2011;196:W123–31.
37. Sugimoto K, Moriyasu F, Saito K, et al. Comparison of Kupffer-phase Sonazoid-enhanced sonography and hepatobiliary-phase gadoxetic acid-enhanced magnetic resonance imaging of hepatocellular carcinoma and correlation with histologic grading. J Ultrasound Med. 2012;31:529–38.
38. Kondo T, Maruyama H, Sekimoto T, et al. Natural history of postvascular-phase iso-enhanced lesions on the sonogram in chronic liver diseases. J Gastroenterol Hepatol. 2014;29:165–72.
39. Korenaga K, Korenaga M, Furukawa M, et al. Usefulness of Sonazoid contrast-enhanced ultrasonography for hepatocellular carcinoma: comparison with pathological diagnosis and super paramagnetic iron oxide magnetic resonance images. J Gastroenterol. 2009;44:733–41.
40. Maruyama H, Takahashi M, Sekimoto T, et al. Heterogeneity of microbubble accumulation: a novel approach to discriminate between well-differentiated hepatocellular carcinomas and regenerative nodules. Ultrasound Med Biol. 2012;38:383–8.
41. Choi BI, Lee JM, Kim TK, et al. Diagnosing borderline hepatic nodules in hepatocarcinogenesis: imaging performance. AJR Am J Roentgenol. 2015;205:10–21.
42. Kudo M, Hatanaka K, Kumada T, et al. Double-contrast ultrasound: a novel surveillance tool for hepatocellular carcinoma. Am J Gastroenterol. 2011;106:368–70.
43. Maruyama H, Takahashi M, Ishibashi H, et al. Ultrasound-guided treatments under low acoustic power contrast harmonic imaging for hepatocellular carcinomas undetected by B-mode ultrasonography. Liver Int. 2009;29:708–14.
44. Miyamoto N, Hiramatsu K, Tsuchiya K, et al. Contrast-enhanced sonography-guided radiofrequency ablation for the local recurrence of previously treated hepatocellular carcinoma undetected by B-mode sonography. J Clin Ultrasound. 2010;38:339–45.
45. Numata K, Morimoto M, Ogura T, et al. Ablation therapy guided by contrast-enhanced sonography with Sonazoid for hepatocellular carcinoma lesions not detected by conventional sonography. J Ultrasound Med. 2008;27:395–406.
46. Minami Y, Kudo M, Hatanaka K, et al. Radiofrequency ablation guided by contrast harmonic sonography using perfluorocarbon microbubbles (Sonazoid) for hepatic malignancies: an initial experience. Liver Int. 2010;30:759–64.
47. Kudo M. New sonographic techniques for the diagnosis and treatment of hepatocellular carcinoma. Hepatol Res. 2007;37(Suppl 2):S193–9.
48. Kudo M, Hatanaka K, Maekawa K. Newly developed novel ultrasound technique, defect reperfusion ultrasound imaging, using Sonazoid in the management of hepatocellular carcinoma. Oncology. 2010;78(Suppl 1):40–5.
49. Ikeda K, Osaki Y, Nakanishi H, et al. Recent progress in radiofrequency ablation therapy for hepatocellular carcinoma. Oncology. 2014;87(Suppl 1):73–7.
50. Meloni MF, Smolock A, Cantisani V, et al. Contrast enhanced ultrasound in the evaluation and percutaneous treatment of hepatic and renal tumors. Eur J Radiol. 2015;84:1666–74.
51. Hiraoka A, Ichiryu M, Tazuya N, et al. Clinical translation in the treatment of hepatocellular carcinoma following the introduction of contrast-enhanced ultrasonography with Sonazoid. Oncol Lett. 2010;1:57–61.
52. Masuzaki R, Shiina S, Tateishi R, et al. Utility of contrast-enhanced ultrasonography with Sonazoid in radiofrequency ablation for hepatocellular carcinoma. J Gastroenterol Hepatol. 2011;26:759–64.
53. Dohmen T, Kataoka E, Yamada I, et al. Efficacy of contrast-enhanced ultrasonography in radiofrequency ablation for hepatocellular carcinoma. Intern Med. 2012;51:1–7.

54. Kudo M. Diagnostic imaging of hepatocellular carcinoma: recent progress. Oncology. 2011;81(Suppl 1):73–85.
55. Inoue T, Kudo M, Hatanaka K, et al. Usefulness of contrast-enhanced ultrasonography to evaluate the post-treatment responses of radiofrequency ablation for hepatocellular carcinoma: comparison with dynamic CT. Oncology. 2013;84(Suppl 1):51–7.
56. Nishigaki Y, Hayashi H, Tomita E, et al. Usefulness of contrast-enhanced ultrasonography using Sonazoid for the assessment of therapeutic response to percutaneous radiofrequency ablation for hepatocellular carcinoma. Hepatol Res. 2015;45:432–40.
57. Inoue T, Minami Y, Chung H, et al. Radiofrequency ablation for hepatocellular carcinoma: assistant techniques for difficult cases. Oncology. 2010;78(Suppl 1):94–101.
58. Andreana L, Kudo M, Hatanaka K, et al. Contrast-enhanced ultrasound techniques for guiding and assessing response to locoregional treatments for hepatocellular carcinoma. Oncology. 2010;78(Suppl 1):68–77.
59. Takahashi M, Maruyama H, Shimada T, et al. Linear enhancement after radio-frequency ablation for hepatocellular carcinoma: Is it a sign of recurrence? Ultrasound Med Biol. 2012;38:1902–10.
60. Maruyama H, Takahashi M, Shimada T, et al. Pretreatment microbubble-induced enhancement in hepatocellular carcinoma predicts intrahepatic distant recurrence after radiofrequency ablation. AJR Am J Roentgenol. 2013;200:570–7.
61. Xia Y, Kudo M, Minami Y, et al. Response evaluation of transcatheter arterial chemoembolization in hepatocellular carcinomas: the usefulness of sonazoid-enhanced harmonic sonography. Oncology. 2008;75(Suppl 1):99–105.
62. Takizawa K, Numata K, Morimoto M, et al. Use of contrast-enhanced ultrasonography with a perflubutane-based contrast agent performed 1 day after transarterial chemoembolization for the early assessment of residual viable hepatocellular carcinoma. Eur J Radiol. 2013;82:1471–80.
63. Kudo M. The 2008 Okuda lecture: management of hepatocellular carcinoma: from surveillance to molecular targeted therapy. J Gastroenterol Hepatol. 2010;25:439–52.
64. Shiozawa K, Watanabe M, Kikuchi Y, et al. Evaluation of sorafenib for hepatocellular carcinoma by contrast-enhanced ultrasonography: a pilot study. World J Gastroenterol. 2012;18:5753–8.
65. Sugimoto K, Moriyasu F, Saito K, et al. Hepatocellular carcinoma treated with sorafenib: early detection of treatment response and major adverse events by contrast-enhanced US. Liver Int. 2013;33:605–15.
66. Abo T, Nanashima A, Tobinaga S, et al. Usefulness of intraoperative diagnosis of hepatic tumors located at the liver surface and hepatic segmental visualization using indocyanine green-photodynamic eye imaging. Eur J Surg Oncol. 2015;41:257–64.
67. Uchiyama K, Ueno M, Ozawa S, et al. Combined intraoperative use of contrast-enhanced ultrasonography imaging using a Sonazoid and fluorescence navigation system with indocyanine green during anatomical hepatectomy. Langenbecks Arch Surg. 2011;396:1101–7.
68. Nanashima A, Tobinaga S, Abo T, et al. Usefulness of Sonazoid-ultrasonography during hepatectomy in patients with liver tumors: a preliminary study. J Surg Oncol. 2011;103:152–7.
69. Arita J, Takahashi M, Hata S, et al. Usefulness of contrast-enhanced intraoperative ultrasound using Sonazoid in patients with hepatocellular carcinoma. Ann Surg. 2011;254:992–9.
70. Mitsunori Y, Tanaka S, Nakamura N, et al. Contrast-enhanced intraoperative ultrasound for hepatocellular carcinoma: high sensitivity of diagnosis and therapeutic impact. J Hepatobiliary Pancreat Sci. 2013;20:234–42.
71. Arita J, Hasegawa K, Takahashi M, et al. Correlation between contrast-enhanced intraoperative ultrasound using Sonazoid and histologic grade of resected hepatocellular carcinoma. AJR Am J Roentgenol. 2011;196:1314–21.
72. Sato K, Tanaka S, Mitsunori Y, et al. Contrast-enhanced intraoperative ultrasonography for vascular imaging of hepatocellular carcinoma: clinical and biological significance. Hepatology. 2013;57:1436–47.
73. Luo W, Numata K, Morimoto M, et al. Three-dimensional contrast-enhanced sonography of vascular patterns of focal liver tumors: pilot study of visualization methods. AJR Am J Roentgenol. 2009;192:165–73.
74. Luo W, Numata K, Morimoto M, et al. Clinical utility of contrast-enhanced three-dimensional ultrasound imaging with Sonazoid: findings on hepatocellular carcinoma lesions. Eur J Radiol. 2009;72:425–31.
75. Numata K, Fukuda H, Ohto M, et al. Evaluation of the therapeutic efficacy of high-intensity focused ultrasound ablation of hepatocellular carcinoma by three-dimensional sonography with a perflubutane-based contrast agent. Eur J Radiol. 2010;75:e67–75.
76. Kunishi Y, Numata K, Morimoto M, et al. Efficacy of fusion imaging combining sonography and hepatobiliary phase MRI with Gd-EOB-DTPA to detect small hepatocellular carcinoma. AJR Am J Roentgenol. 2012;198:106–14.
77. Makino Y, Imai Y, Ohama H, et al. Ultrasonography fusion imaging system increases the chance of radiofrequency ablation for hepatocellular carcinoma with poor conspicuity on conventional ultrasonography. Oncology. 2013;84(Suppl 1):44–50.
78. Min JH, Lim HK, Lim S, et al. Radiofrequency ablation of very-early-stage hepatocellular carcinoma inconspicuous on fusion imaging with B-mode US: value of fusion imaging with contrast-enhanced US. Clin Mol Hepatol. 2014;20:61–70.
79. Numata K, Fukuda H, Morimoto M, et al. Use of fusion imaging combining contrast-enhanced ultrasonography with a perflubutane-based contrast agent and contrast-enhanced computed tomography for the evaluation of percutaneous radiofrequency ablation of hypervascular hepatocellular carcinoma. Eur J Radiol. 2012;81:2746–53.
80. Shindoh J, Seyama Y, Umekita N. Three-dimensional staining of liver segments with an ultrasound contrast agent as an aid to anatomic liver resection. J Am Coll Surg. 2012;215:e5–10.
81. Bota S, Piscaglia F, Marinelli S, et al. Comparison of international guidelines for noninvasive diagnosis of hepatocellular carcinoma. Liver Cancer. 2012;1:190–200.
82. Tanaka H, Iijima H, Nouso K, et al. Cost-effectiveness analysis on the surveillance for hepatocellular carcinoma in liver cirrhosis patients using contrast-enhanced ultrasonography. Hepatol Res. 2012;42:376–84.
83. Shiozawa K, Watanabe M, Takayama R, et al. Evaluation of local recurrence after treatment for hepatocellular carcinoma by contrast-enhanced ultrasonography using Sonazoid: comparison with dynamic computed tomography. J Clin Ultrasound. 2010;38:182–9.